

Ab initio mechanism for efficient population of triplet states in cytotoxic sulfur substituted DNA bases: the case of 6-Thioguanine.

Lara Martínez-Fernández,^a Leticia González^b and Inés Corral ^{*a}

^aDepartamento de Química, Facultad de Ciencias, Universidad Autónoma de Madrid, Campus de Excelencia UAM-CSIC, Módulo 13, Cantoblanco, 28049-Madrid, Spain.
E-mail: ines.corral@uam.es. Fax: (+34) 914975238

^bInstitute of Theoretical Chemistry, University of Vienna, Währingerstrasse 17, 1090 Vienna, Austria.

Additional Computational details

6-Thioguanine (6-TG) UV absorption spectrum has been calculated using the ground state equilibrium structure optimized with the complete active space self-consistent field (CASSCF) method,¹ and the ANO-L basis set contracted as C,O [4s3p2d]/S[5s4p2d]/H[3s2p].² A (12,10) active space, including π orbitals and a sulfur lone-pair, was used for the geometry optimization (see Figure S1). Vertical energies were calculated following the MS-CASPT2//SA-CASSCF/ANO-L (multistate second order perturbation theory on state average complete active space self-consistent field wavefunctions)^{3,4} approach over 8 singlet and 7 triplet roots, with an increased (14,12) active space, containing an *s* Rydberg orbital, (see Figure S1). A real level shift⁵ parameter of 0.3 au was added to the zero order Hamiltonian to prevent the appearance of intruder states. The performance of TD-DFT⁶ functionals, B3LYP⁷⁻⁹ and CAMB3LYP¹⁰, was assessed using MS-CASPT2 vertical energies as a benchmark. TD-CAMB3LYP provides singlet vertical energies in good agreement with CASPT2 (absolute errors ca. 0.1 eV) but provide too low energies for the triplets, with differences that can amount to 0.9 eV, (Compare Tables S1-S2). The assignment of the electronic spectra of 6-thioguanosine in different environments by Reichardt et al.¹¹ was compared to that obtained from our own PBE0¹² calculations on the gas phase B3LYP/6-311++G(d,p) optimized structure. Using this geometry we are able to reproduce their vacuo vertical energies while small energy differences, that amount to 0.1 eV, arise when solvent (water) solute interactions through the PCM model are considered which we ascribe to geometric changes induced by the solvent that we did not take into account. From these calculations, we conclude that both the nucleobase and the nucleoside show the same character for their lower lying electronic excited states and similar excitation energies.

Minimum energy paths (MEPs) in Figures S3-S6 were computed following the intrinsic reaction coordinate (IRC) algorithm¹³ to locate energy-accessible stationary points (Table S5 and Figure S2). These calculations were performed using the CASSCF/6-31G* protocol with the same (12,10) active space employed for the optimization of the ground state (see Figure S1) and the number of roots necessary. The geometry of the stationary points was reoptimized using an ANO-RCC triple ζ quality basis set. The contraction scheme used for this basis set was C,O [3s2p1d]/S[4s3p1d]/H[2s1p].

Singlet-singlet and Singlet-triplet minimum energy crossing points were optimized at the CASSCF(12,10)/6-31G* level of theory using as starting geometries those extracted from the MEPs and the Franck-Condon (FC) structure, respectively.

Final energies were refined at MS-CASPT2//CASSCF(14,12)/ANO-L level of theory (Table S4). Initial singlet and triplet CASSCF(14,12) wavefunctions were obtained through state-average calculations using 3 and 2 roots, respectively.

The inclusion of dynamical correlation generally increases the energy gap between the states involved in the surface crossings (ca. 0.70 eV). In these cases, the geometries were slightly modified until an energy difference smaller than 0.2 eV between the two intersecting states was reached at MS-CASPT2 level of theory. Unfortunately, in the specific case of the ${}^1(\pi\pi^*/S_0)$ conical intersection this led to a degeneracy point lying 0.2 eV above the FC spectroscopic state. Therefore, the MS-CASPT2 potential energy surface around the CASSCF conical intersection was explored by hand until a new degeneracy point of the potential energy surface was found lying below the FC point.

The probability of intersystem crossing along the MEP was evaluated by calculating spin-orbit coupling terms at critical points of the PES, namely FC geometry, singlet minima and singlet/triplet minimum energy crossing points. These calculations were performed using SA-CASSCF(12,10)/ANO-RCC wavefunctions including five singlet and five triplet states.

MS-CASPT2 vertical spectrum calculations, stationary point optimizations, spin-orbit couplings and final energies calculations were performed with the version 7.4 of MOLCAS¹⁴ program. GAUSSIAN 09¹⁵ was employed for calculating TD-DFT vertical spectra, minimum energy paths and optimizing singlet-singlet conical intersections. The optimization of singlet-triplet minimum energy crossing points was done with MOLPRO 2006.¹⁶

References

- 1 B. O. Roos, in *Ab initio Methods in Quantum Chemistry II*, ed. K. P. Lawley, Wiley, Chichester, 1987.
- 2 P. O. Widmark, P. Å. Malmqvist and B. O. Roos, *Theor. Chim. Acta*, 1990, **77**, 291.
- 3 K. Andersson, P. Å. Malmqvist and B. O. Roos, *J. Chem. Phys.*, 1992, **96**, 1218.
- 4 J. Finley, P. Å. Malmqvist, B. O. Roos and L. Serrano-Andrés, *Chem. Phys. Lett.*, 1998, **288**, 299.
- 5 B. O. Roos and K. Andersson, *Chem. Phys. Lett.*, 1995, **245**, 215.
- 6 E. Runge and E. K. U. Gross, *Phys. Rev. Lett.*, 1984, **52**, 997.
- 7 A. D. Becke, *J. Chem. Phys.*, 1993, **98**, 5648.
- 8 A. D. Becke, *Phys. Rev. A*, 1988, **38**, 3098.
- 9 C. Lee, W. Yang and R. G. Parr, *Phys. Rev. B*, 1988, **37**, 785.
- 10 T. Yanai, D. P. Tew and N. C. Handy, *Chem. Phys. Lett.*, 2004, **393**, 51.
- 11 C. Reichardt, C. Guo and C. E. Crespo-Hernández, *J. Phys. Chem. B*, 2011, **115**, 3263.
- 12 C. Adamo and V. Barone, *J. Chem. Phys.*, 1999, **110**, 6158.
- 13 A. Migani and M. Olivucci, in *Conical Intersections: Electronic Structure, Dynamics and Spectroscopy*, Vol. 15, ed. W. Domcke, D. Yarkony, H. Köppel, World Scientific, Singapore, 2004.
- 14 F. Aquilante, L. De Vico, N. Ferré, G. Ghigo, P. Å. Malmqvist, P. Neogrády, T. B. Pedersen, M. Pitoňák, M. Reiher, B. O. Roos, L. Serrano-Andrés, M. Urban, V. Veryazov and R. Lindh, *J. Comput. Chem.*, 2010, **31**, 224.
- 15 M. J. Frisch, G. W. Trucks, H. B. Schlegel, G. E. Scuseria, M. A. Robb, J. R. Cheeseman, G. Scalmani, V. Barone, B. Mennucci, G. A. Petersson, H. Nakatsuji, M. Caricato, X. Li, H. P. Hratchian, A. F. Izmaylov, J. Bloino, G. Zheng, J. L. Sonnenberg, M. Hada, M. Ehara, K. Toyota, R. Fukuda, J. Hasegawa, M. Ishida, T. Nakajima, Y. Honda, O. Kitao, H. Nakai, T. Vreven, J. A. Montgomery, Jr., J. E. Peralta, F. Ogliaro, M. Bearpark, J. J. Heyd, E. Brothers,

- K. N. Kudin, V. N. Staroverov, R. Kobayashi, J. Normand, K. Raghavachari, A. Rendell, J. C. Burant, S. S. Iyengar, J. Tomasi, M. Cossi, N. Rega, J. M. Millam, M. Klene, J. E. Knox, J. B. Cross, V. Bakken, C. Adamo, J. Jaramillo, R. Gomperts, R. E. Stratmann, O. Yazyev, A. J. Austin, R. Cammi, C. Pomelli, J. W. Ochterski, R. L. Martin, K. Morokuma, V. G. Zakrzewski, G. A. Voth, P. Salvador, J. J. Dannenberg, S. Dapprich, A. D. Daniels, Ö. Farkas, J. B. Foresman, J. V. Ortiz, J. Cioslowski and D. J. Fox, *Gaussian 09, Revision A.1*, Gaussian, Inc., Wallingford CT, 2009.
- 16 H.-J. Werner, P. J. Knowles, R. Lindh, F. R. Manby, M. Schütz, P. Celani, T. Korona, G. Rauhut, R. D. Amos, A. Bernhardsson, A. Berning, D. L. Cooper, M. J. O. Deegan, A. J. Dobbyn, F. Eckert, C. Hampel and G. Hetzer, A.W. Lloyd, S. J. McNicholas, W. Meyer and M. E. Mura, A. Nicklass, P. Palmieri, R. Pitzer, U. Schumann, H. Stoll, A. J. Stone, R. Tarroni and T. Thorsteinsson, *MOLPRO version 2006.1, a package of ab initio programs*, <http://www.molpro.net>, 2006.

Table S1. MS-CASPT2//CASSCF(14,12)/ANO-L absorption spectrum of 6-thioguanine.

State	CI Coeff.	ΔE [eV]	Oscillator strength	State	CI Coeff.	ΔE [eV]
$^1(n_S\pi^*_{CS})$	0.91	3.36	0.0000	$^3(\pi\pi^*_{CS})$	-0.86	3.10
$^1(\pi\pi^*_{CS})$	0.83	4.05	0.5352	$^3(n_S\pi^*_{CS})$	-0.91	3.31
$^1(\pi\pi^*)$	0.86	4.90	0.1440	$^3(\pi\pi^*)$	-0.86	4.24
$^1(n_S\pi^*)$	-0.80	5.07	0.0070	$^3(\pi_{CS}\pi^*_{CS})$	-0.72	5.05
$^1(\pi Ryd_{(s)})$	-0.71	5.16	0.0154	$^3(n_S\pi^*)$	-0.84	5.10
$^1(n_S Ryd_{(s)})$	-0.80	5.23	0.0254	$^3(\pi Ryd_{(s)})$	-0.73	5.17
$^1(\pi_{CS}\pi^*_{CS})$	-0.67	5.80	0.0112	$^3(n_S Ryd_{(s)})$	-0.79	5.18

Table S2. TD-CAMB3LYP/6-311G(3df,2p) absorption spectrum of 6-thioguanine.

State	Coeff.	ΔE [eV]	Oscillator strength	State	Coeff.	ΔE [eV]
$^1(n_S\pi^*_{CS})$	0.70	3.27	0.0000	$^3(\pi\pi^*_{CS})$	0.69	2.50
$^1(\pi\pi^*_{CS})$	0.67	4.15	0.3193	$^3(n_S\pi^*_{CS})$	0.69	2.93
$^1(\pi\pi^*)$	0.55	4.81	0.1798	$^3(\pi\pi^*)$	0.53	3.61
$^1(n_S\pi^*)$	0.50	5.37	0.0066	$^3(\pi_{CS}\pi^*_{CS})$	0.57	4.17
$^1(\pi Ryd_{(s)})$	0.64	5.03	0.0013	$^3(n_S\pi^*)$	0.56	5.32
$^1(n_S Ryd_{(s)})$	0.45	5.41	0.0180	$^3(\pi Ryd_{(s)})$	0.63	4.98
$^1(\pi_{CS}\pi^*_{CS})$	0.60	5.70	0.0474	$^3(n_S Ryd_{(s)})$	0.53	5.22

Table S3. TD-B3LYP/6-311G(3df,2p) absorption spectrum of 6-thioguanine.

State	Coeff.	ΔE [eV]	Oscillator strength	State	Coeff.	ΔE [eV]
$^1(n_S\pi^*_{CS})$	0.70	3.11	0.0000	$^3(\pi\pi^*_{CS})$	0.69	2.59
$^1(\pi\pi^*_{CS})$	0.62	4.00	0.2176	$^3(n_S\pi^*_{CS})$	0.70	2.79
$^1(\pi\pi^*)$	0.64	4.34	0.1547	$^3(\pi\pi^*)$	0.64	3.48
$^1(n_S\pi^*)$	0.70	4.23	0.0023	$^3(\pi_{CS}\pi^*_{CS})$	0.64	4.04
$^1(\pi Ryd_{(s)})$	0.70	4.49	0.0103	$^3(n_S\pi^*)$	0.69	4.19
$^1(n_S Ryd_{(s)})$	0.67	4.60	0.0255	$^3(\pi Ryd_{(s)})$	0.65	4.43
$^1(\pi_{CS}\pi^*_{CS})$	0.65	5.24	0.0466	$^3(n_S Ryd_{(s)})$	0.67	4.51

Table S4. MS-CASPT2//CASSCF(14,12)/ANO-L energies (in eV) for the lowest lying singlet and triplet states at the optimized critical points along the deactivation pathway of 6-thioguanine relative to the ground state.

Structure	State	ΔE [eV]	State	ΔE [eV]
$^1(n_S\pi^*_{CS})_{min}$	gs	1.07	$^3(n_S\pi^*_{CS})$	3.08
	$^1(n_S\pi^*_{CS})$	3.14		3.12
	$^1(\pi\pi^*_{CS})$	4.13		
$^1(\pi\pi^*_{CS})_{min}$	gs	1.45	$^3(\pi\pi^*_{CS})$	3.60
	$^1(\pi\pi^*_{CS})$	3.80		3.99
	$^1(n_S\pi^*_{CS})$	3.91		
$^1(\pi\pi^*_{CS})/{}^1(n_S\pi^*_{CS})_{CI}$	gs	1.55	$^3(\pi\pi^*_{CS})$	3.70
	$^1(\pi\pi^*_{CS})$	3.86		
	$^1(n_S\pi^*_{CS})$	3.97		
$^1(\pi\pi^*_{CS})/S_0\text{ CI}$	gs	3.71	$^3(\pi\pi^*_{CS})$	3.36
	$^1(\pi\pi^*_{CS})$	3.82		
	$^1(n_S\pi^*_{CS})$	5.41		
$^1(n\pi^*_{CS})/S_0\text{ CI}$	gs	4.59	$^3(\pi\pi^*_{CS})$	4.73
	$^1(n_S\pi^*_{CS})$	4.97		
	$^1(\pi\pi^*_{CS})$	5.72		
${}^3(n_S\pi^*_{CS})_{min}$	gs	0.88	${}^3(\pi\pi^*_{CS})$	3.02
	${}^1(n_S\pi^*_{CS})$	3.18		
	${}^1(\pi\pi^*_{CS})$	3.91		
${}^3(\pi\pi^*_{CS})_{TS}$	gs	1.55	${}^3(\pi\pi^*_{CS})$	3.59
	${}^1(\pi\pi^*_{CS})$	4.12		
	${}^1(n_S\pi^*_{CS})$	4.37		
${}^3(\pi\pi^*_{CS})_{min1}$	gs	1.45	${}^3(\pi\pi^*_{CS})$	3.41
	${}^1(\pi\pi^*_{CS})$	3.97		
	${}^1(n_S\pi^*_{CS})$	4.11		
${}^3(\pi\pi^*_{CS})_{min2}$	gs	0.88	${}^3(\pi\pi^*_{CS})$	3.02
	${}^1(n_S\pi^*_{CS})$	3.18		
	${}^1(\pi\pi^*_{CS})$	3.91		
${}^3(\pi\pi^*_{CS})/{}^3(n_S\pi^*_{CS})_{CI}$	gs	0.87	${}^3(n_S\pi^*_{CS})$	3.07
	${}^1(n_S\pi^*_{CS})$	3.19		
	${}^1(\pi\pi^*_{CS})$	3.91		
${}^1(n_S\pi^*_{CS})/{}^3(\pi\pi^*_{CS})_{ISC}$	gs	0.82	${}^3(\pi\pi^*_{CS})$	3.03
	${}^1(n_S\pi^*_{CS})$	3.14		
	${}^1(\pi\pi^*_{CS})$	3.95		
${}^1(\pi\pi^*_{CS})/{}^3(n\pi^*_{CS})_{ISC}$	gs	1.55	${}^3(\pi\pi^*_{CS})$	3.70
	${}^1(\pi\pi^*_{CS})$	3.86		
	${}^1(n_S\pi^*_{CS})$	3.97		

Table S5. Cartesian coordinates (in Å) of the CASSCF optimized structures for the relevant points in the deactivation mechanism of 6-thioguanine.

Atom	X	Y	Z
FC			
H	-2.364357	0.744097	-0.084506
H	-2.719688	-2.657519	0.050851
H	-3.446813	-1.252081	0.510343
H	2.218466	-2.538989	-0.034943
H	3.853963	-0.593074	0.000693
C	-1.509000	-1.095310	-0.014869
C	-0.368626	1.076522	0.010331
C	0.815110	0.268910	0.008468
C	0.692148	-1.092087	-0.012114
C	2.791243	-0.491740	0.000583
N	-1.497244	0.266684	-0.009987
N	-2.762197	-1.672366	-0.076920
N	-0.452089	-1.826127	-0.010179
N	2.150180	0.627788	0.016037
N	1.959053	-1.584859	-0.015137
S	-0.498381	2.707598	0.020381

Atom	X	Y	Z
${}^1(n_S\pi^*_{CS})_{min}$			
H	-2.359530	0.660853	-0.471351
H	-2.731071	-2.650032	0.102927
H	-3.427891	-1.242859	0.592310
H	2.236076	-2.530346	0.053579
H	3.855209	-0.581637	-0.024589
C	-1.519407	-1.091865	0.005734
C	-0.359731	1.061558	-0.181705
C	0.811621	0.265535	-0.084897
C	0.692378	-1.083449	-0.004427
C	2.790104	-0.489010	-0.033926
N	-1.545746	0.288835	-0.035037
N	-2.780035	-1.664280	-0.039147
N	-0.472661	-1.817507	0.057116
N	2.144118	0.631033	-0.097843
N	1.969444	-1.577275	0.026307
S	-0.441112	2.707889	0.493980

Atom	X	Y	Z
${}^1(\pi\pi^*_{\text{CS}})_{\text{min}}$			
H	-2.356848	0.858839	-0.037473
H	-2.863349	-1.964463	-0.813864
H	-3.069116	-2.275766	0.756215
H	2.202827	-2.557521	0.146995
H	3.825474	-0.626734	-0.095305
C	-1.594744	-0.991418	0.393072
C	-0.327329	1.029599	-0.083605
C	0.804526	0.297261	0.036232
C	0.642845	-1.136902	0.140742
C	2.763377	-0.507436	-0.043587
N	-1.505875	0.347461	-0.008484
N	-2.853576	-1.552158	0.102084
N	-0.443674	-1.793722	0.252538
N	2.155061	0.620641	-0.073626
N	1.927633	-1.609537	0.064802
S	-0.445466	2.749301	-0.377707

Atom	X	Y	Z
${}^1(\pi\pi^*_{\text{CS}})/{}^1(n_S\pi^*_{\text{CS}})_{\text{CI}}$			
H	-2.359219	0.880600	0.015621
H	-2.836640	-1.941906	-0.867845
H	-3.105550	-2.291581	0.687014
H	2.230508	-2.522321	0.355997
H	3.833491	-0.615524	-0.109611
C	-1.608459	-0.995046	0.416534
C	-0.330736	1.005619	-0.083378
C	0.798074	0.268742	-0.101286
C	0.644361	-1.153703	0.107921
C	2.768990	-0.507744	-0.088390
N	-1.507173	0.363051	0.114212
N	-2.858744	-1.550547	0.060014
N	-0.443848	-1.795187	0.311313
N	2.151752	0.609896	-0.201645
N	1.939725	-1.623933	0.046261
S	-0.454763	2.757029	-0.303706

Atom	X	Y	Z
${}^1(\pi\pi^*_{\text{CS}})/S_0 \text{ Cl}$			
H	2.20365400	0.84841100	1.31016700
H	3.20516900	-1.81128600	-0.66694400
H	3.75898700	-0.42426100	0.13825200
H	-1.69969400	-2.60736200	-0.66392400
H	-3.65939800	-1.20241900	0.15363900
C	-2.64288100	-0.86520100	0.14782400
C	-0.86975000	0.27887500	0.36593000
C	-0.46890300	-0.96449800	-0.21932300
C	1.71952700	-0.63234000	0.04297400
C	0.21617900	1.16313800	0.73332200
N	-2.24522500	0.28050000	0.58474000
N	-1.62444400	-1.66581000	-0.35568400
N	0.75607700	-1.40055700	-0.46099600
N	1.47069900	0.46396100	0.75777900
N	3.01758200	-1.07116800	-0.02585500
S	-0.07228700	2.19178600	-0.63721500

Atom	X	Y	Z
${}^1(n\pi^*_{\text{CS}})/S_0 \text{ Cl}$			
H	-2.378535	0.818297	-0.106125
H	-2.821066	-2.605830	0.303490
H	-3.619837	-1.148694	0.023459
H	2.200120	-2.131055	0.897351
H	3.796219	-0.336776	0.010836
C	-1.582423	-1.059507	-0.024683
C	-0.389913	0.963905	-0.414786
C	0.739438	0.133746	-0.800777
C	0.654069	-0.968522	0.075985
C	2.737055	-0.333164	-0.159626
N	-1.599399	0.276654	-0.411077
N	-2.789393	-1.688113	-0.080367
N	-0.504119	-1.720212	0.252962
N	2.068494	0.583769	-0.776392
N	1.926696	-1.378161	0.298226
S	0.424360	1.481105	1.270557

Atom	X	Y	Z
${}^3(n_S\pi^*_{CS})_{min}$			
H	-2.384783	0.711098	-0.290451
H	-2.713666	-2.655311	0.138441
H	-3.441243	-1.233833	0.532323
H	2.229705	-2.535174	0.075718
H	3.853942	-0.589005	-0.011854
C	-1.516987	-1.092120	-0.024203
C	-0.353028	1.059716	-0.218538
C	0.812324	0.272131	-0.083915
C	0.692155	-1.087649	-0.005975
C	2.789066	-0.492625	-0.025553
N	-1.519321	0.267578	-0.086807
N	-2.770003	-1.679161	-0.055923
N	-0.462091	-1.821155	0.031921
N	2.149496	0.628186	-0.092365
N	1.965835	-1.582252	0.024694
S	-0.469633	2.717020	0.451519

Atom	X	Y	Z
${}^3(\pi\pi^*_{CS})_{TS}$			
H	-2.372929	0.809032	-0.006250
H	-3.466881	-1.220129	-0.141645
H	-2.597421	-2.603125	-0.108650
H	2.257361	-2.542587	0.291228
H	3.817460	-0.591148	-0.146369
C	-1.568086	-1.011606	0.533650
C	-0.391516	1.031337	-0.157048
C	0.785898	0.260686	-0.019158
C	0.658033	-1.163911	0.178667
C	2.752980	-0.509842	-0.083189
N	-1.534468	0.277150	-0.072116
N	-2.760728	-1.728416	0.344982
N	-0.405789	-1.823759	0.393647
N	2.102803	0.603576	-0.164479
N	1.953937	-1.622759	0.083268
S	-0.424233	2.660674	-0.451163

Atom	X	Y	Z
${}^3(\pi\pi^*_{\text{CS}})_{\text{min}1}$			
H	-2.374320	0.854088	-0.005170
H	-2.859686	-1.851519	-0.854412
H	-3.016977	-2.364284	0.672945
H	2.211891	-2.555345	0.210984
H	3.813318	-0.618782	-0.122846
C	-1.606762	-0.981804	0.449023
C	-0.368160	1.072616	-0.102937
C	0.798170	0.285259	0.000981
C	0.642630	-1.138905	0.159816
C	2.750257	-0.518253	-0.065425
N	-1.517698	0.349255	0.007491
N	-2.841633	-1.560245	0.106867
N	-0.436600	-1.794363	0.326572
N	2.118295	0.609887	-0.127977
N	1.930790	-1.613986	0.082241
S	-0.381747	2.713826	-0.379124

Atom	X	Y	Z
${}^3(\pi\pi^*_{\text{CS}})_{\text{min}2}$			
H	-2.383614	0.710961	-0.285374
H	-2.712852	-2.654081	0.133707
H	-3.433654	-1.236246	0.544146
H	2.227729	-2.535439	0.077974
H	3.853091	-0.595643	-0.005397
C	-1.514780	-1.090824	-0.027146
C	-0.351495	1.061695	-0.221362
C	0.816798	0.276986	-0.088354
C	0.693375	-1.089179	-0.010972
C	2.788815	-0.496633	-0.023803
N	-1.517070	0.267248	-0.086576
N	-2.771077	-1.677243	-0.056876
N	-0.462486	-1.818458	0.028341
N	2.147110	0.628450	-0.092133
N	1.964358	-1.581865	0.023819
S	-0.482479	2.717715	0.449037

Atom	X	Y	Z
${}^3(\pi\pi^*_{cs})/{}^3(n_s\pi^*_{cs})_{ci}$			
H	-2.357209	0.771354	0.467204
H	-3.492785	-1.068142	-0.565473
H	-2.833917	-2.537449	-0.213201
H	2.138339	-2.609055	-0.248732
H	3.835574	-0.725318	-0.064894
C	-1.563699	-1.035534	0.017592
C	-0.314451	1.053804	0.364846
C	0.825345	0.227050	0.148337
C	0.650741	-1.119718	-0.025563
C	2.774262	-0.595026	-0.018086
N	-1.511337	0.319530	0.194762
N	-2.845781	-1.565019	0.012133
N	-0.538821	-1.802507	-0.111200
N	2.174257	0.541627	0.148351
N	1.909749	-1.650445	-0.127064
S	-0.364788	2.755428	-0.194989

Atom	X	Y	Z
${}^1(n_s\pi^*_{cs})/{}^3(\pi\pi^*_{cs})_{sc}$			
H	-2.378376	0.690480	-0.375758
H	-2.731516	-2.660040	0.086699
H	-3.435404	-1.253561	0.586865
H	2.233969	-2.538236	0.059631
H	3.860754	-0.593759	-0.010554
C	-1.520297	-1.095499	-0.006101
C	-0.358542	1.065820	-0.176667
C	0.820336	0.276254	-0.073969
C	0.696750	-1.092586	-0.014983
C	2.795762	-0.495115	-0.024306
N	-1.535974	0.281822	-0.034788
N	-2.779782	-1.671089	-0.041522
N	-0.467714	-1.826824	0.033712
N	2.151132	0.633334	-0.076510
N	1.970584	-1.581613	0.011209
S	-0.459934	2.748057	0.416220

Atom	X	Y	Z
${}^1(\pi\pi^*_{CS})/{}^3(n_S\pi^*_{CS})_{ISC}$			
H	-2.359219	0.880600	0.015621
H	-2.836640	-1.941906	-0.867845
H	-3.105550	-2.291581	0.687014
H	2.230508	-2.522321	0.355997
H	3.833491	-0.615524	-0.109611
C	-1.608459	-0.995046	0.416534
C	-0.330736	1.005619	-0.083378
C	0.798074	0.268742	-0.101286
C	0.644361	-1.153703	0.107921
C	2.768990	-0.507744	-0.088390
N	-1.507173	0.363051	0.114212
N	-2.858744	-1.550547	0.060014
N	-0.443848	-1.795187	0.311313
N	2.151752	0.609896	-0.201645
N	1.939725	-1.623933	0.046261
S	-0.454763	2.757029	-0.303706

Figure S1. CASSCF optimized molecular orbitals of the (14,12) active space used for the calculation of the vertical absorption spectrum of 6-thioguanine. Framed in black, the orbitals comprised in the (12,10) active space used for geometry optimizations and minimum energy path calculations.

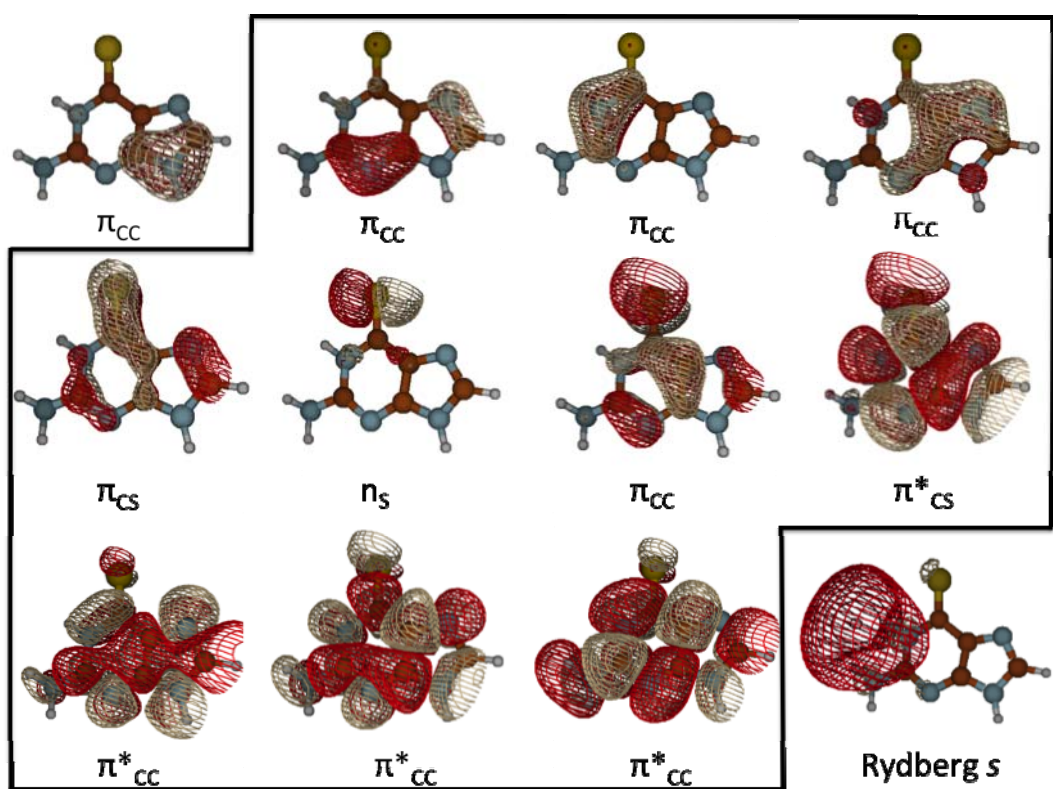
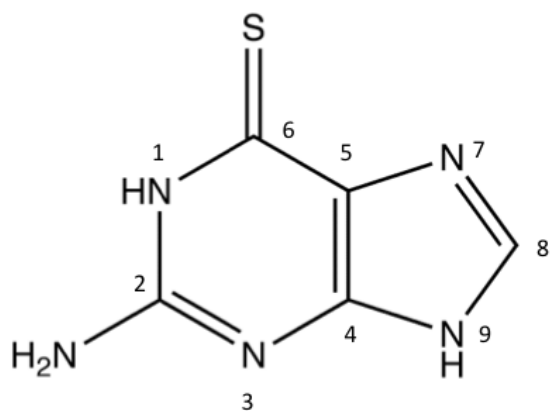
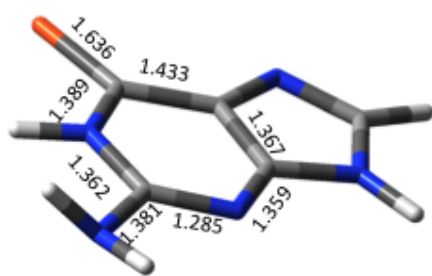


Figure S2. Representative distances in angstroms and dihedral angles in degrees for the CASSCF optimized structures for the relevant points in the deactivation mechanism of 6-thioguanine.

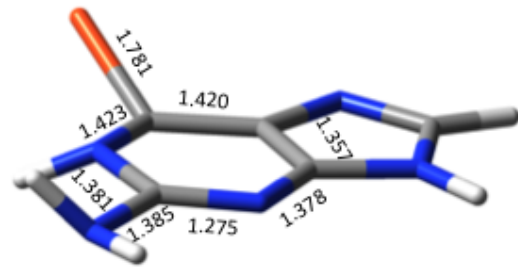


$d(SC_6C_5C_4) = -179.5^\circ$
 $d(C_6C_5C_4N_3) = -1.2^\circ$
 $d(C_6N_1C_2N_3) = -0.5^\circ$



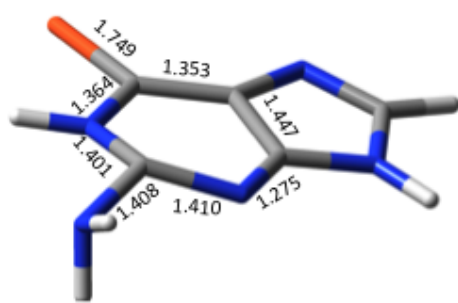
FC

$d(SC_6C_5C_4) = 148.9^\circ$
 $d(C_6C_5C_4N_3) = -3.2^\circ$
 $d(C_6N_1C_2N_3) = 7.5^\circ$



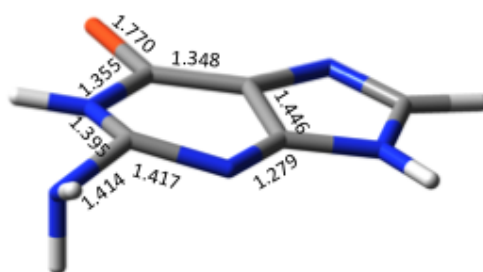
$^1(n_S\pi_{CS}^*)_{min}$

$d(SC_6C_5C_4) = -173.8^\circ$
 $d(C_6C_5C_4N_3) = -6.8^\circ$
 $d(C_6N_1C_2N_3) = -23.2^\circ$



$^1(\pi\pi_{CS}^*)_{min}$

$d(SC_6C_5C_4) = 179.8^\circ$
 $d(C_6C_5C_4N_3) = -0.1^\circ$
 $d(C_6N_1C_2N_3) = -10.1^\circ$



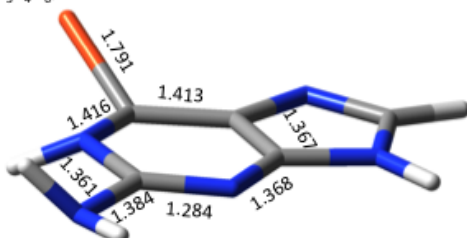
$^1(\pi\pi_{CS}^*)/1(n_S\pi_{CS}^*)_{cl}$

$d(SC_6C_5C_4) = 104.3^\circ$
 $d(C_6C_5C_4N_3) = 0.1^\circ$
 $d(C_2N_3C_4N_6) = -19.5^\circ$



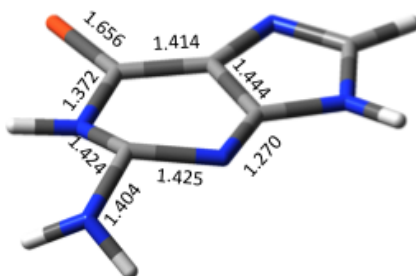
${}^1(n_S\pi_{CS}^*)/S_0$ Cl

$d(SC_6C_5C_4) = 148.9^\circ$
 $d(C_6C_5C_4N_3) = -3.9^\circ$
 $d(C_2N_3C_4N_6) = 5.9^\circ$



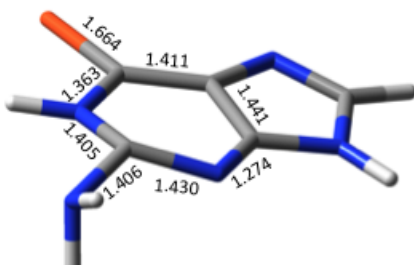
${}^1(n_S\pi_{CS}^*)/S_0$ Cl

$d(SC_6C_5C_4) = -177.4^\circ$
 $d(C_6C_5C_4N_3) = -8.4^\circ$
 $d(C_2N_3C_4N_6) = -34.1^\circ$



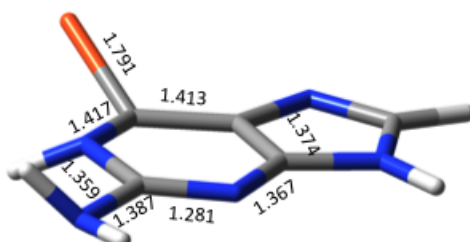
${}^3(n_S\pi_{CS}^*)_{min}$

$d(SC_6C_5C_4) = -176.2^\circ$
 $d(C_6C_5C_4N_3) = -6.1^\circ$
 $d(C_6N_1C_2N_3) = -23.4^\circ$



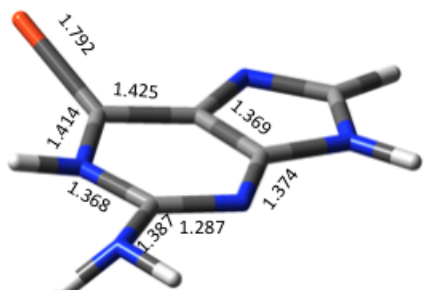
${}^3(n_S\pi_{CS}^*)_{min1}$

$d(SC_6C_5C_4) = 148.9^\circ$
 $d(C_6C_5C_4N_3) = -4.0^\circ$
 $d(C_6N_1C_2N_3) = 6.2^\circ$



${}^3(n_S\pi_{CS}^*)_{min2}$

$d(SC_6C_5C_4) = 148.7^\circ$
 $d(C_6C_5C_4N_3) = 4.9^\circ$
 $d(C_6N_1C_2N_3) = -5.1^\circ$



${}^3(n_S\pi_{CS}^*)/{}^3(\pi\pi_{CS}^*)_{Cl}$

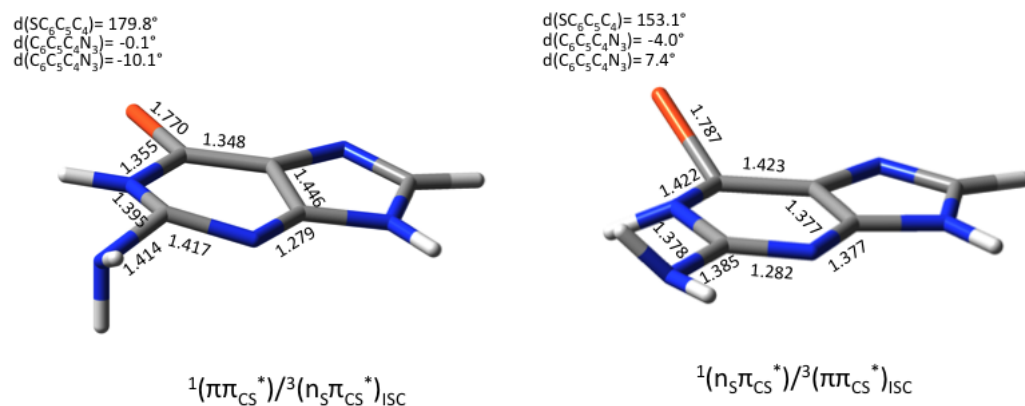


Figure S3. CASSCF energy profiles for the lowest-lying singlet states along the minimum energy path of the ${}^1(n_s\pi_{CS}^*)$ state from the FC structure.

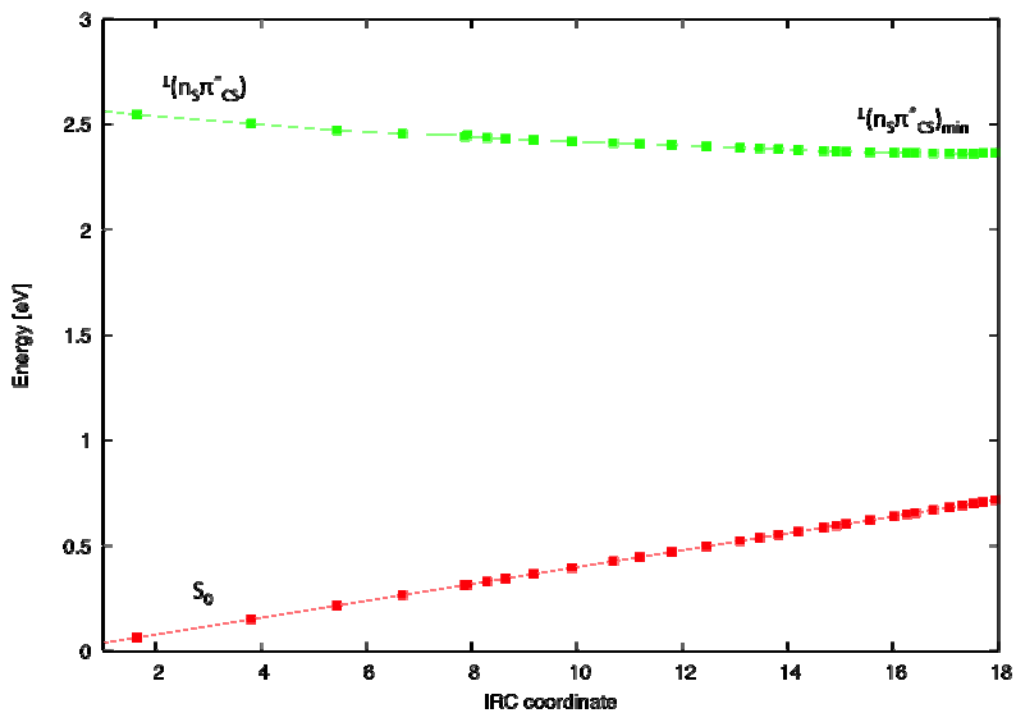


Figure S4. CASSCF energy profiles for the lowest-lying singlet states along the minimum energy path of the ${}^1(\pi\pi^*_{CS})$ state from the FC structure.

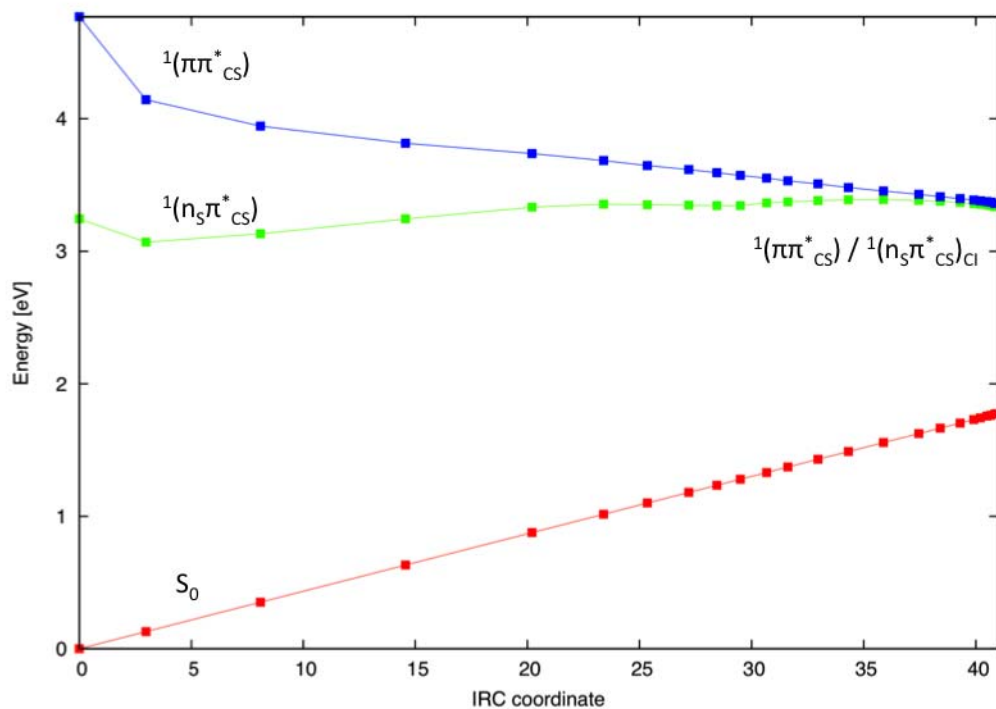


Figure S5. CASSCF energy profiles for the lowest-lying singlet states along the minimum energy path of the ${}^1(n_s\pi^*_{CS})$ state (left) and ${}^1(\pi\pi^*_{CS})$ state (right) from the ${}^1(\pi\pi^*_{CS}) / {}^1(n_s\pi^*_{CS})_{CI}$ structure.

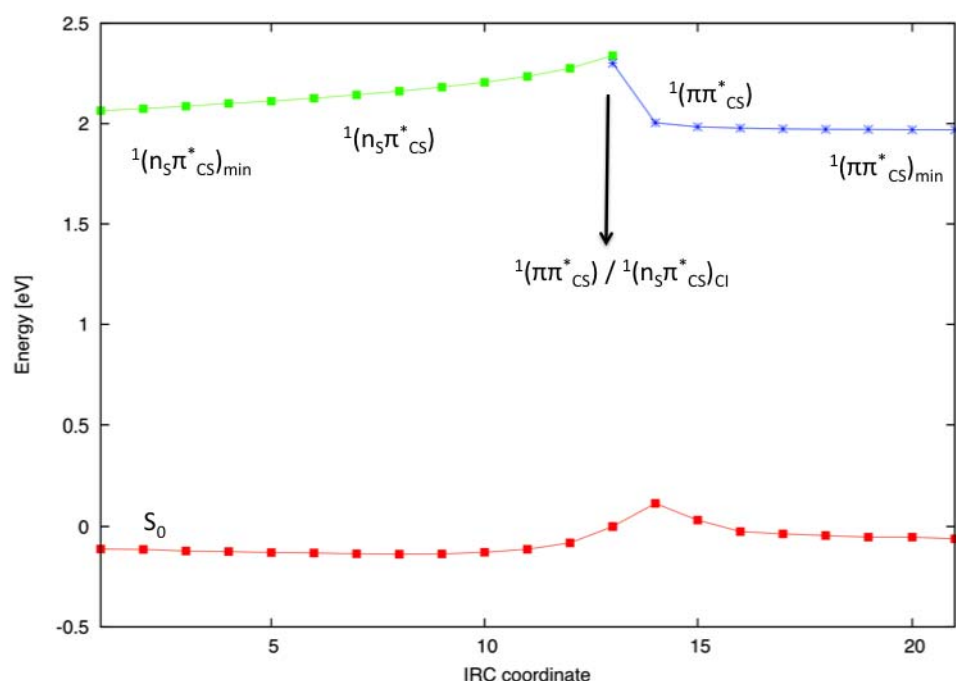


Figure S6. CASSCF energy profiles for the lowest-lying triplet states along the minimum energy path of the ${}^3(n_s\pi^*_{CS})$ state from the ${}^1(\pi\pi^*_{CS})/{}^3(n_s\pi^*_{CS})$ structure.

